Available online at www.sciencedirect.com
ScienceDirect
Journal of Power Sources 169 (2007) 177–183
JOURNAL OF POWER SOURCES
www.elsevier.com/locate/jpowsour

Development of biogas reforming Ni-La-Al catalysts for fuel cells☆

M. Benito*, S. García, P. Ferreira-Aparicio, L. García Serrano, L. Daza

Instituto de Catálisis y Petroleoquímica (CSIC), C/ Marie Curie 2, Campus Cantoblanco, 28049 Madrid, Spain

Available online 30 January 2007

Abstract

In this work, the results obtained for Ni-La-Al catalysts developed in our laboratory for biogas reforming are presented. The catalyst 5% Ni/5% La_2O_3-γ-Al_2O_3 has operated under kinetic control conditions for more than 40 h at 700 °C and feeding CH_4/CO_2 ratio 1/1, similar to the composition presented in biogas streams, being observed a stable behaviour.

Reaction parameters studied to evaluate the catalyst activity were H_2/CO and CH_4/CO_2 conversion ratio obtained. On the basis of a CH_4 conversion of 6.5%, CH_4/CO_2 conversion ratio achieved 0.48 and H_2/CO ratio obtained was 0.43. By comparison of experimental results to equilibrium prediction for such conditions, is detectable a lower progress of reverse water gas shift reaction. This fact increases the H_2/CO ratio obtained and therefore the hydrogen production. The higher H_2/CO and a CH_4/CO_2 conversion ratio in comparison to CH_4 one close to equilibrium is due to the carbon deposits gasification which avoids catalyst deactivation. A thermodynamic analysis about the application of dry and combined methane reforming to hydrogen production for fuel cells application is presented. Data obtained by process simulation considering a Peng–Robinson thermodynamic model, allows optimizing process conditions depending on biogas composition.

Keywords: Biogas; Reforming; Hydrogen; Fuel cell; Processor; Methane

1. Introduction

The problems associated to the extraction capacity and refine of petroleum together to the excessive increment of the fossil fuels consumption, it has increased the possibility of using renewable energy sources as well as the revalorizarion of remainders able to generate fuels such as methane for the energy production.

This solution could reduce the external energy dependence and it would favor the development of the local economy through the concept of decentralized generation, reducing the emissions of greenhouse gases to the atmosphere.

In Europe, the use and production of biogas as a source of primary energy is experiencing to get the objective of production of 15 millions of TOE in the 2010.

The biogas produced in anaerobic digestors could contain methane concentrations of until 80% in volume, and its quality would depend on its origin (drain, anaerobic digestion of residual waters or treatment of residuals).

Traditionally biogas has been burned in internal combustion engines for the electricity production and heat, but its potential use in fuel cells could increase its electric efficiency, especially in applications at low scale, diminishing the NO_x emissions to the atmosphere [1–5].

For biogas reforming in mixtures with considerable contents of CO_2, a process that get special attention is the dry gas reforming or carbon dioxide reforming. This process is of particular interest, since it allows to take advantage of the CO_2 presented in biogas composition as oxidizer in the gas reforming [6–8]. For biogas streams with CO_2/CH_4 ratios less than unit, it is required the addition of an alternative oxidizer for the production of synthesis gas [9,10].

One of the main limitations of dry gas reforming technology application is the development of catalysts able to avoid the deposition of carbon on the active phase to increase their period of useful life [11–14].

In this work, the results obtained for a catalyst developed in our laboratory for the methane reforming with CO_2 are presented. The comparison of the experimental results versus

☆ This paper presented at the 2nd National Congress on Fuel Cells, CONAPPICE 2006.

* Corresponding author. Tel.: +34 91 5854946; fax: +34 91 5854760.
E-mail address: mjbenito@icp.csic.es (M. Benito).

0378-7753/$ – see front matter © 2007 Elsevier B.V. All rights reserved.
doi:10.1016/j.jpowsour.2007.01.046

thermodynamic calculations will allow discern the participation of the different reactions involved in the mechanism.

2. Experimental

2.1. Catalyst preparation

A series of catalysts were prepared by the method of impregnation in aqueous solution with different Ni content (5%, 10%, 15%) using $Ni(NO_3)_2{\bullet}6H_2O$ as a precursor of the active phase. Once impregnated the active phase on modified with 3% and 5% of La_2O_3, respectively, γ-Al_2O_3, these samples were dried at 110 °C during 12 h and calcined at 750 °C during 2 h. The samples obtained were denoted as *x*NiAl*y*La, where *x* is the Ni weight concentration expressed in percent, and *y* represents La weight concentration expressed in percent. A catalyst denoted as 5NiAl was prepared as a reference for catalytic activity measurements.

2.2. Catalyst characterisation

The samples denoted as 5NiAl3La and 5NiAl5La, respectively, were characterised by X-ray diffraction, N_2 adsorption and chemical analysis by emission spectroscopy of plasma coupled inductively. TG experiments have been performed on samples with different nickel content (5NiAl3La, 10NiAl3La, 15NiAl3La), respectively.

The chemical composition of the catalysts, was analyzed by inductively coupled plasma atomic emission spectroscopy (ICP-AES), using an Optima 3300DV Perkin-Elmer equipment.

Catalysts were characterized by XRD and the diffractograms were recorded following a step-scanning procedure (step-size 0.02°, 2θ scanning from 4° to 100° by a Seifert 3000P diffractometer coupled to an acquisition data system). The samples were analysed between 4° and 100° by using the radiation Cu Kα ($\lambda = 0.15481$ nm). The identification of the crystallographic phases was performed by using the software PDFWIN. This software is based on diffraction data from International Centre for Diffraction Data. To calculate the particle size from XRD patterns, the Scherrer equation was applied.

Nitrogen adsorption–desorption isotherms were obtained at −196 °C using an automatic system Micromeritcs ASAP 2100. The catalysts samples were previously out-gassed at 150 °C for 12 h. BET surface areas were calculated from isotherms by adjusting to Brunauer–Emmet–Teller mathematical expression.

TG experiments of the catalysts samples were performed in a thermobalance Mettler Toledo (TGA/SDTA851e). A sample (20 mg) was placed in an alumina recipient and submitted to a gas stream (40% H_2–40% N_2). The experiment temperature was increased at 10 °C min^{-1} to achieve 800 °C.

The characterization of the catalyst after the reaction has been carried out by scanning electron microscopy using a microscope Hitachi S-3000N with analyser for disperse energy of X-rays. In order to analyse the carbon deposits on the samples, a layer of gold was deposited and analysed by X-ray diffraction (Sputter Coater SC-502).

The catalytic tests were carried out in a fixed bed tubular reactor of quartz (6 mm) in a commercial system Microactivity Reference (PID Eng & Tech) connected on-line to a gas chromatograph Agilent 6890 provided of a detector of thermal conductivity and another of flame ionization. For the separation of the reaction products two columns have been used in series (Chromosorb 102 and Porapak Q). Prior to reaction, the catalyst (20 mg) was meshed between 0.42 and 0.50 mm and it was reduced in situ for 2 h at 700 °C in hydrogen. The reaction was carried out at 700 °C, feeding a stream of 100 ml min^{-1} of methane and carbon dioxide ($CH_4/CO_2 = 1{:}1$ mol) and 10 ml min^{-1} of N_2 used as internal reference.

The activity of the catalyst has been studied in function of the reaction temperature in the temperature range 550–800 °C, with increments of 50 °C at atmospheric pressure.

3. Results and discussion

3.1. Characterisation

3.1.1. XRD characterisation

XRD diffractograms obtained on γ-Al_2O_3 modified with different lanthana contents (Al3La, Al5La) are represented in Fig. 1.

Lanthanum phases La_2O_3 (05-0602, JCPDS), $LaAlO_3$ (85-1071, JCPDS) and $LaAl_{12}O_{19}$ (77-0335, JCPDS) were not detected, but its presence has been reported by other authors [15].

Diffractograms obtained from catalysts with a 5NiAl3La and 5NiAl5La are represented in Fig. 2.

The lanthanum increment on the support does not affect to the diffraction patterns obtained from calcined catalysts. It is noteworthy that nickel oxide and nickel metallic were not detected which indicates a high dispersion degree of nickel on the support.

3.1.2. Textural analysis

Fig. 3a shows the N_2 isotherm adsorption curves for Al3La and Fig. 4a for Al5La, respectively. Both N_2 isotherms are IV type and present hysteresis loop H2 type associated to the presence of pores that constitutes a neck bottle produced as

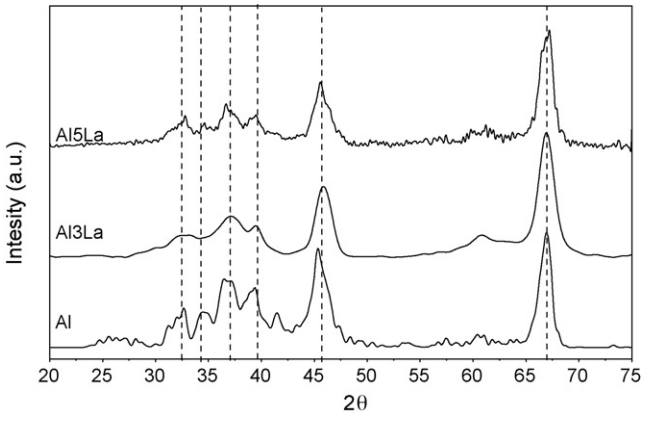

Fig. 1. XRD diffractograms obtained from alumina support modified by La_2O_3 addition.

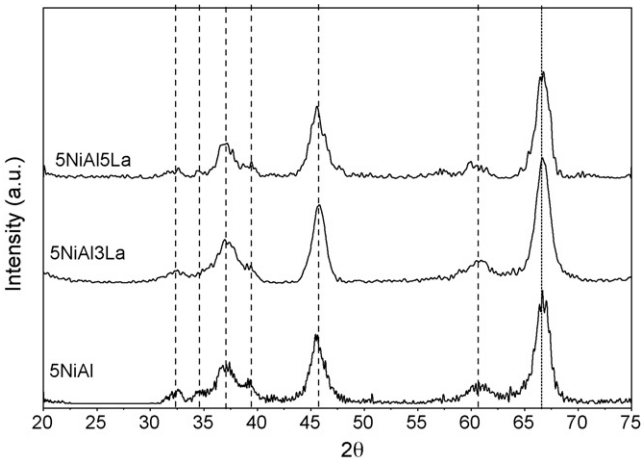

Fig. 2. XRD diffractograms obtained from 5% Ni supported on alumina support modified by 3% and 5% of La_2O_3 addition.

consequence of lanthana deposition on alumina structure (Figs. 3b and 4b).

The increase of lanthanum content, produces a slight decrease of BET surface area and pore volume, from 138 $m^2\,g^{-1}$ and

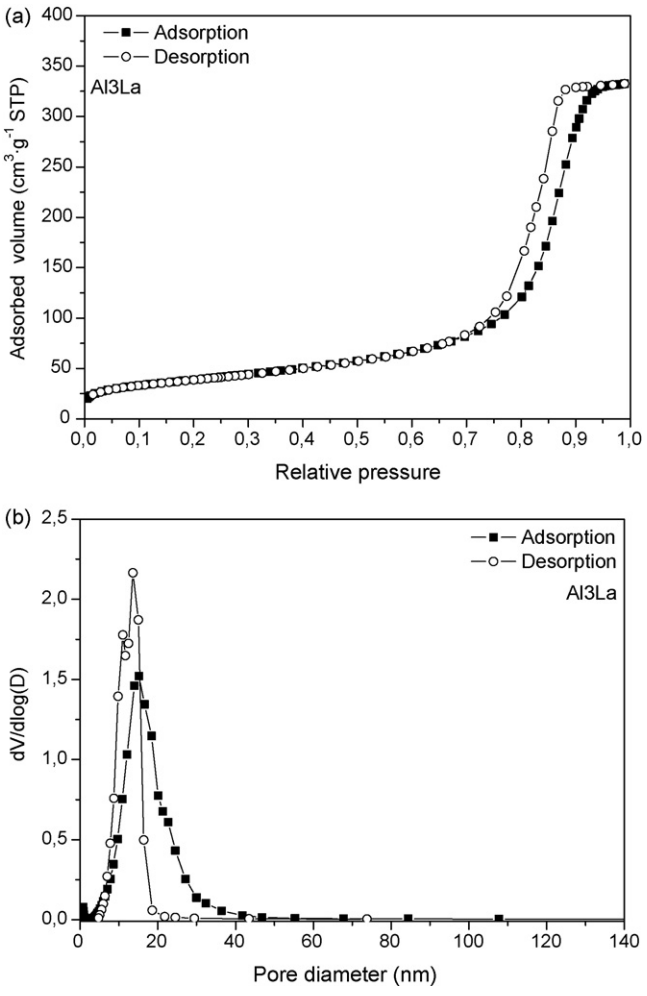

Fig. 3. (a) N_2 adsorption isotherm obtained for Al3La. (b) Pore diameter distribution obtained for Al3La.

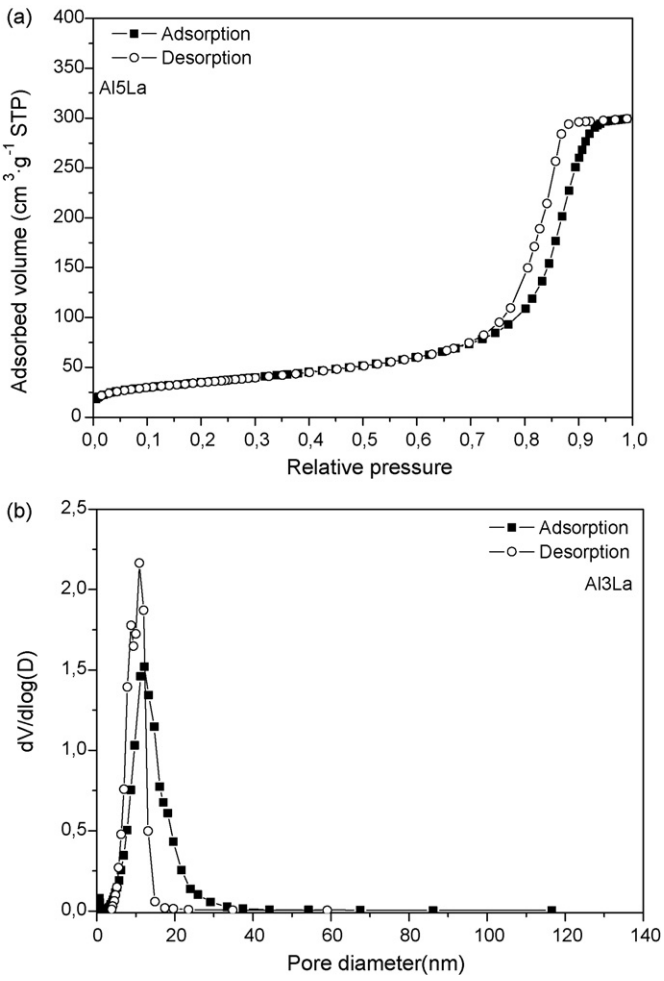

Fig. 4. (a) N_2 adsorption isotherm obtained for Al5La. (b) Pore diameter distribution obtained for Al5La.

0.5 $cm^3\,g^{-1}$ for Al3La to 125 $m^2\,g^{-1}$ and 0.45 $cm^3\,g^{-1}$ for Al5La.

3.1.3. Thermogravimetric analysis

In Fig. 5a are represented the thermogravimetric curves and in Fig. 5b the derivative curves (DTG) that correspond to Al3La, 5NiAl3La, 10NiAl3La and 15NiAl3La, respectively, where the nickel content has been increased from 0% to 15%. The increase of active phase content produces a slight increment of free nickel (600 °C). At temperature higher than 700 °C start to reduce $NiAl_2O_4$. The presence of this phase stabilizes the low size Ni metallic crystallites formation in reduction conditions, which has a positive influence on reaction behaviour [16]. This mass loss is more evidenced in samples with higher nickel content.

The decrease of the reduction temperature for samples impregnated with lanthana has been reported in literature due to the formation of a $LaNiO_3$ phase which decomposes at 400 °C [17]. Nevertheless, this fact was not detected in our experiments.

3.2. Catalytic activity tests

In order to analyse the influence of the $CH_4/CO_2/H_2O$ composition on the methane conversion, a thermodynamic analysis

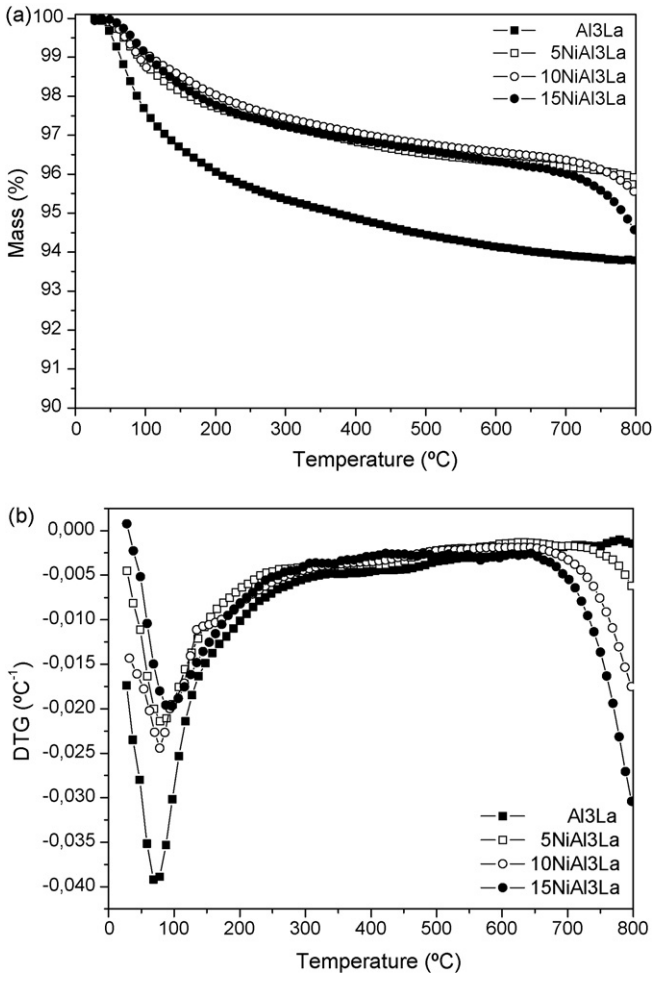

Fig. 5. (a) TG curves for Al3La supported catalysts with different Ni content. (b) DTG curves for Al3La supported catalysts with different Ni content.

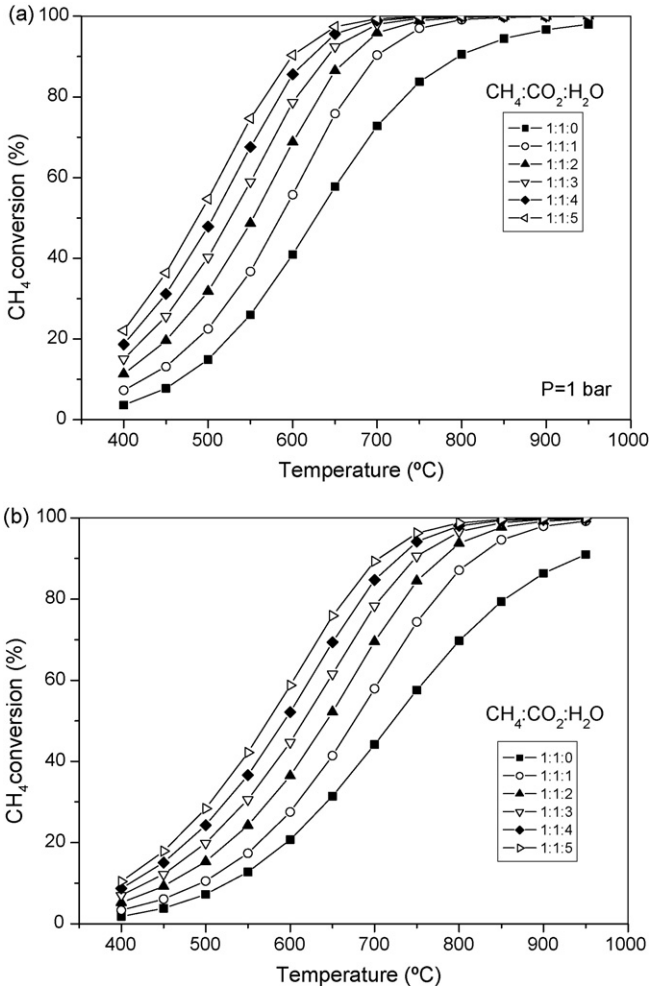

Fig. 6. (a) Equilibrium conversion of CH_4 in function of the temperature at 1 bar. (b) Equilibrium conversion of CH_4 in function of the temperature at 5 bar.

was performed. Fig. 6a shows the methane conversion in the equilibrium in function of the temperature for several molar ratios of $CH_4/CO_2/H_2O$ in the feed at 1 bar. The calculations were carried out with the simulation of ASPEN PLUS software, under the model of physical properties of Peng–Robinson. It was kept in mind the reactions of methane reforming with carbon dioxide (1), steam reforming (2) and the water gas shift reaction (3), simulating the equilibrium in a Gibbs reactor.

$$CH_4 + CO_2 \leftrightarrows 2H_2 + 2CO, \quad \Delta H^{\circ}_{298K} = 247\,\text{kJ mol}^{-1} \qquad (1)$$

$$CH_4 + H_2O \leftrightarrows 3H_2 + CO, \quad \Delta H^{\circ}_{298K} = 206\,\text{kJ mol}^{-1} \qquad (2)$$

$$CO + H_2O \leftrightarrows H_2 + CO_2, \quad \Delta H^{\circ}_{298K} = -41\,\text{kJ mol}^{-1} \qquad (3)$$

For all compositions the conversion increases with the temperature and it is almost completed from 900 °C, although the addition of water diminishes this temperature to 750 °C, displacing the curves toward lower temperatures. This simulation allows settle- down the conditions so that the reactor works far from the equilibrium ones and determines that the analysis of catalytic activity are correct and were obtained in kinetic control. The increase of the pressure of the system to 5 bar, produces a shift of all the conversion curves at equilibrium toward higher temperatures (Fig. 6b). Although when the pressure was 1 bar, total conversion of methane was achieved at 950 °C, even working under conditions of having reforming dry, when operation pressure is 5 bar it reaches 90%. The trend when the concentration of water increases it is similar to the previous case, although even with the addition of water it is necessary to operate at 900 °C to reach conversion values close to 100%.

It is known that strong metal support interactions (SMSI) can have a great influence on catalytic activity [18]. The high intrinsic catalytic activity of catalysts promoted with La_2O_3 can be associated to the absence of an alkaline in the catalyst on account of La_2O_3 presents a moderately alkaline character. Basic promoters inhibit the surface carbon formation but on the contrary decrease the catalytic activity in a significant manner [19].

The decrease of hydrogen production could be due to an active sites blocking by carbon deposits formation, that proceeds from methane decomposition or Boudouard's reaction.

3.2.1. *Effect of lanthana content on the support*

CH_4 and CO_2 conversion for the samples with an increasing lanthana content (5NiAl, 5NiAl3La and 5NiAl5La) are shown in Figs. 7 and 8, respectively.

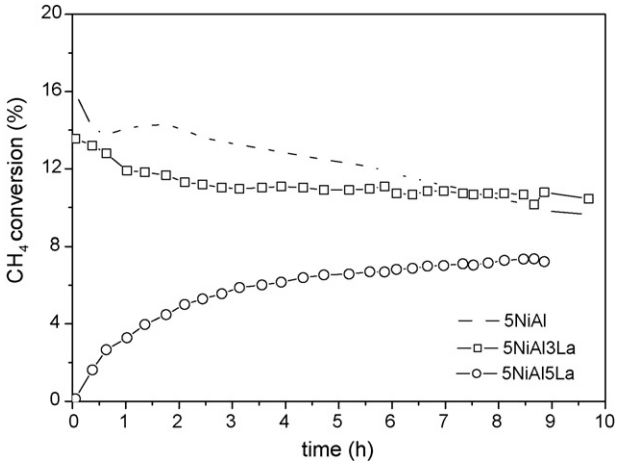

Fig. 7. CH_4 conversion vs. time at 700 °C for 5% Ni supported on Al, Al3La and Al5La.

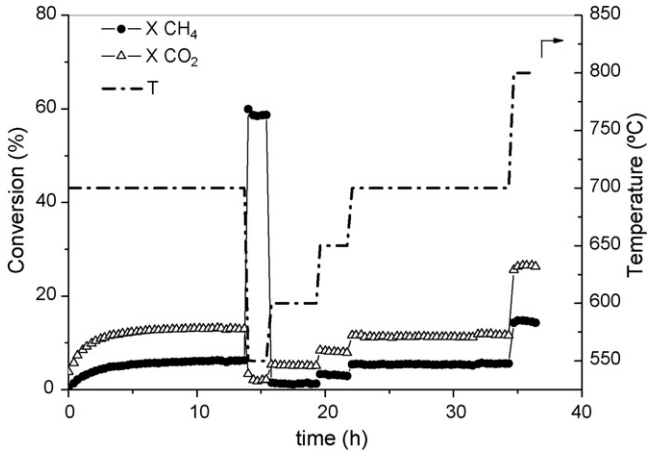

Fig. 9. CH_4, CO_2 conversion vs. time–temperature.

$NiAl_2O_4$ phase favors the resistance to carbon deposits formation but presents lower activity than other Ni catalyst precursors calcined at lower temperatures. This activity decreases with the lanthana content. On the other hand, lanthanum promoted catalysts present much higher stability. In reaction conditions, nickel particles are partially covered by $La_2O_2CO_3$ which are produced by La_2O_3 and CO_2 interaction [20].

Catalytic activity takes place in Ni-$La_2O_2CO_3$ inter-phase, while oxy-carbonate species participate directly reacting with carbon deposited on the metal, recovering nickel activity. This is the limit stage for these catalysts. The increase of reaction rate at the beginning of the experiment suggests a slow process where an equilibrium in $La_2O_2CO_3$ and for others carbonaceous species on the surface nickel crystallites is established. $La_2O_2CO_3$ phase has a moderate stability and can be partially decomposed at reaction temperatures [21,22]. This species can be considered as an oxygen dynamic tampon. Species –C–C– are removed by oxidation reactions to produce CO. The observed stable behaviour is due to an equilibrium achieved between carbon species formation on nickel crystallites and removing rate of such species by oxidation reaction with the participation of $La_2O_2CO_3$ and formate species.

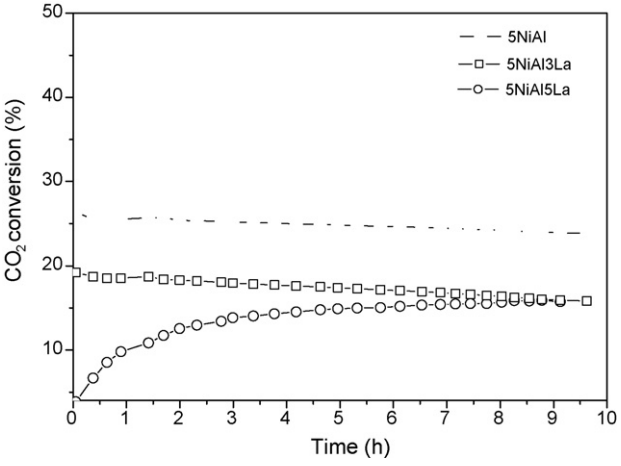

Fig. 8. CO_2 conversion vs. time at 700 °C for 5% Ni supported on Al, Al3La and Al5La.

The reduction pretreatment influence at 700 or 800 °C has been studied. The reduction pre-treatment has a low influence in the initial reaction rate, but its influence in steady-state period is negligible. In this type of catalyst, there is a strong trend to establish a surface structure in reaction conditions [20].

In Fig. 9 are represented the conversion of CH_4 and of CO_2 versus reaction time, and the temperature for the catalyst 5NiAl5La synthesized in our laboratory. To check the stability of the catalyst, it has worked under kinetic control conditions (conversion less than 10%). It is observed how the catalyst, after a period of stabilization under reaction conditions at 700 °C, reached a value of conversion of 6.45%, which remained stable after 14 h in reaction conditions. When the temperature decreases, the conversion of CO and CO_2 also decreases remaining stable in the time in the temperature range 550–800 °C.

The CO_2 conversion was higher than CH_4 conversion on account of the CO_2 was converted due to water gas shift reverse reaction that would produce the appearance of water in the distribution of the reaction products. Nevertheless, the increase hoped in the production of water does not take place, from this, it was deduced that the increase of the conversion of CO_2 could be due to another reaction, such as the gasification of carbonaceous deposits.

The possibility of gasification of the carbonaceous deposits is suggested from the results represented in Fig. 10 in which the H_2/CO ratio is represented versus time and reaction temperature. This ratio reaches the value of 0.43 at 700 °C which stays stable in the time, and after being submitted to the temperature cycle. The biggest production of CO with regard to the H_2 (more than 2) could be explained due to the Boudouard's reverse reaction or the gasification of the carbonaceous deposits with CO_2.

In Fig. 11, the conversion of CO_2, the ratios XCO_2/XCH_4 and H_2/CO were represented in function of the calculated conversion of CH_4 from the thermodynamic equilibrium at 700 °C and 1 bar. In this graph, the experimental values for the catalyst 5NiAl5La under the suitable reaction conditions are also represented.

It has observed how the ratio between the CH_4 and CO_2 conversion was slightly higher than the equilibrium predicted

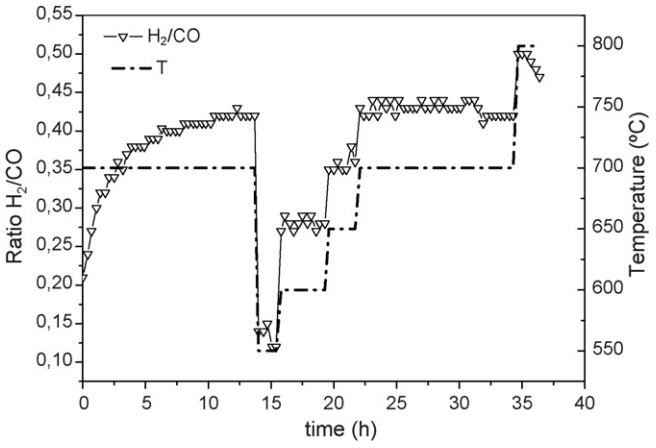

Fig. 10. H_2/CO ratio obtained in function of time–temperature.

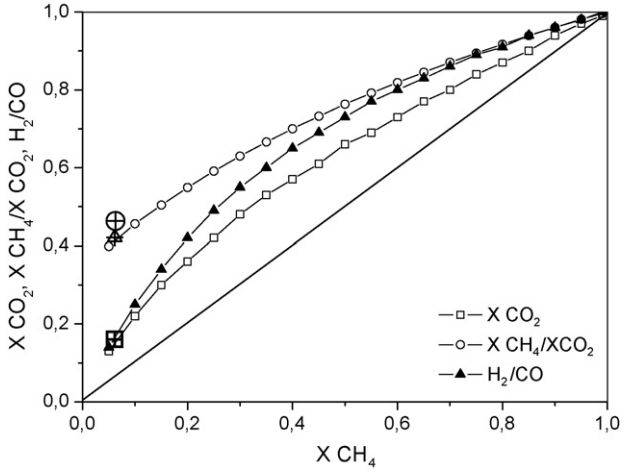

Fig. 11. Comparison of experimental results vs. thermodynamic predictions.

one, what would suppose (in theory) the decomposition of CH_4 on the active phase, promoting the deposition of carbon. However, the ratio H_2/CO obtained is quite higher than the equilibrium predicted one, which indicates that the participation of the reverse water gas shift reaction is very small. From this

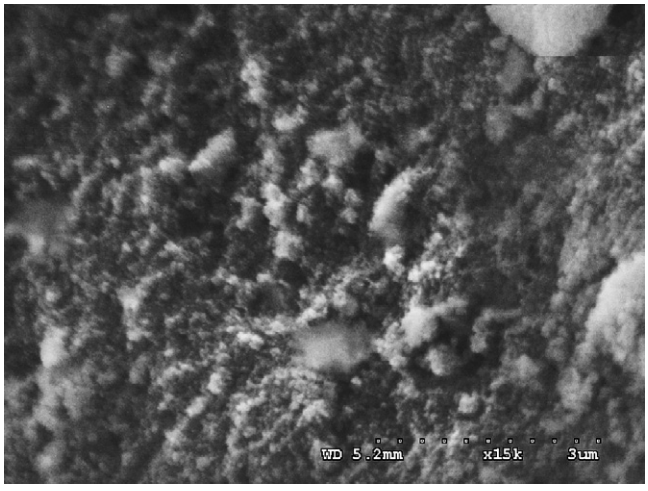

Fig. 12. SEM image of 5NiAl5La catalyst after 40 h in reaction conditions.

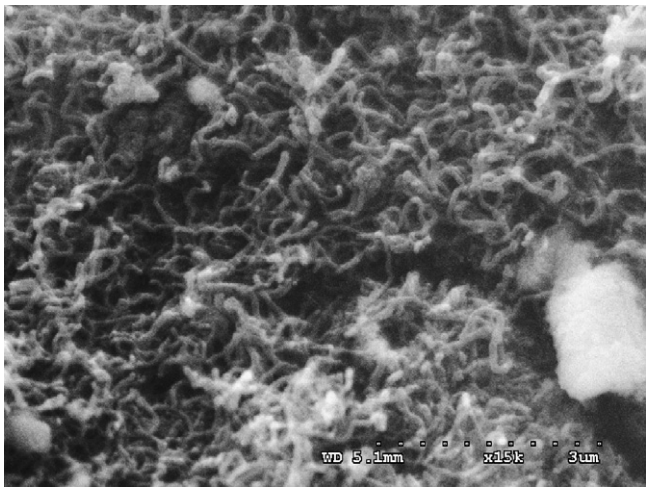

Fig. 13. SEM image of a catalyst after 40 h in reaction conditions with carbon deposits.

standpoint it could conclude that the absence of deactivation phenomena can be due to the gasification of the carbon deposits with CO_2 (Boudouard's reverse reaction) produced by CH_4 decomposition.

In Fig. 12 is presented the image by scanning electronic microscopy (SEM) of the catalyst tested after 40 h in reaction. From the image it is observed that the surface of the catalyst remains free of carbon deposits, not being detected the presence of carbon filaments whose formation is characteristic in this type of systems (Fig. 13). The results of characterization obtained by scanning microscopy, corroborate the hypothesis of the carbon deposits gasification as the responsible for the maintenance in the stability of the catalytic activity for the studied catalyst.

4. Conclusions

The catalyst 5NiAl5La synthesized in our laboratory and operating under conditions of kinetic control (conversion less than 10%) showed a total stability after 40 h under dry reforming conditions in CH_4:CO_2 ratio 1:1, similar to the usually presented ones in the biogas streams. The equilibrium between deposition and gasification of the carbon deposits could be responsible for the great stability of the system.

Acknowledgments

This work has been carried out with the economic support of the projects ENERCAM-CM S-0505/ENE-304 and PROFIT FIT-310200-2004-168 in collaboration with the company Aguas de Murcia, to which the authors express its gratefulness for the on trust in them and the financial support.

References

[1] S. Baron, Biofuels and Their Use in Fuel Cells, Imperial College, 2004.
[2] CADDET Japanese National Team, Fuel Cell CHP Using Biogas from Brewery Effluent, 1999.
[3] A. Effendi, Z.-G. Zhang, K. Hellgardt, K. Honda, T. Yoshida, Catal. Today 77 (2002) 181.

[4] Q. Jing, H. Lou, J. Fei, Z. Hou, X. Zheng, Int. J. Hydrogen Energy 29 (2004) 1245.
[5] S. Mullik, P. Pietrogrande, D. Warren, Performance Evaluation for the 40 kW Fuel Cell Power Plant Utilizing a Generic Landfill Gas Feedstock, KTI-Kinetics Technology International Corporation, 1986.
[6] J.R.H. Ross, A.N.J. van Keulen, M.E.S. Hegarty, K. Seshan, Catal. Today 30 (1996) 193.
[7] J.R. Rostrup-Nielsen, J. Sehested, Adv. Catal. 47 (2002) 65.
[8] J.R. Rostrup-Nielsen, T. Rostrup-Nielsen, CATTECH 6 (2002) 150.
[9] G.F. Froment, J. Mol. Catal. A 163 (2000) 147.
[10] H. Roh, K. Jun, W. Dong, S. Park, Y. Baek, Catal. Lett. 74 (2001) 31.
[11] A. Sacco, A.H. Geurts, G.A. Jablonski, S. Lee, R.A. Gately, J. Catal. 119 (1989) 322.
[12] E.E. Wolf, F. Alfani, Catal. Rev. 24 (1982) 329.
[13] E.T.C. Vogt, A.J. van Dillen, J.W. Geus, Stud. Surf. Sci. (1987) 221.
[14] D.S. Williams, R. Möller, H.J. Grabke, High Temp. Sci. 14 (1981) 33.
[15] R. Blom, I.M. Dahl, A. Slagtern, B. Sortland, A. Spjelkavik, E. Tangstad, Catal. Today 21 (1994) 535.
[16] A.M. Gadalla, B. Bower, Chem. Eng. Sci. 43 (11) (1988) 3049.
[17] Z. Cheng, Q. Wu, J. Li, Q. Zhu, Catal. Today 30 (1996) 147.
[18] M. Boudart, G. Djéga-Mariadassou, Kinetiks of Heterogeneous Catalytic Reactions, Princeton Univ. Press, Princeton, 1984, p. 201.
[19] D.E. Ridler, M.V. Twigg, in: M.V. Twigg (Ed.), Catalyst Handbook, Londres, Wolfe, 1989, p. 225.
[20] X.E. Verykios, Int. J. Hidrogen Energy 28 (2003) 1045.
[21] S. Bernal, G.A. Martin, P. Morl, V. Perrichon, Catal. Lett. 6 (1990) 231.
[22] O.V. Kryolov, A. Kh Mamedov, S.R. Mirzabekova, Ind. Eng. Chem. 34 (1995) 474.